MELCOR

Further Development Phase 2: 2017–2021

Author and Co-author(s)	Bernd S. Jäckel, Leticia Fernandez-Moguel, Terttaliisa Lind
Institution	Paul-Scherrer-Institut
Address	5232 Villigen PSI
Phone, E-mail, Internet address	+41 56 310 2658, bernd.jaeckel@psi.ch, www.psi.ch/sacre
Duration of the Project	2017–2021

ABSTRACT

Full scale experiments conducted in 2011 and 2012 at the Sandia National Laboratories in the Sandia Fuel Project, three QUENCH bundle tests at KIT as well as many separate effect tests in various labs have shown that nitrogen plays an active role in the degradation process of the Zr-based fuel cladding materials. Cladding oxidation in the presence of nitrogen may lead to accelerated loss of the only barrier for the fission product release in case of a spent fuel storage accident. To account for the effect of nitrogen in the cladding degradation, PSI together with KIT has conducted an experimental programme during the years 2014 and 2015.

More than 70 separate effect tests were conducted by a PhD student of PSI at KIT. The results of the tests provide a data base sufficient enough for the development of a nitriding and re-oxidation model to describe the accelerated degradation of Zr-based cladding materials under air ingress conditions in the temperature range 900–1200 °C. The samples were analyzed not only for the mass gain during exposure to subsequently oxygen, nitrogen, and again oxygen, but also for the composition after the tests using a combined metallographic and image analysis. The conceptual model for nitriding includes formation of ZrO_2 and oxygen stabilized α-Zirconium (α-Zr(O)) during pre-oxidation in oxygen, fast nitriding and slow nitriding during the exposure to nitrogen, the effect of breakaway oxidation, and the fast re-oxidation of ZrN and remaining metal.

A standalone computer code to describe the nitriding reactions was developed based on the separate effect tests conducted at KIT. In the present report, the model concept and the first calculations are presented for all phases of pre-oxidation, nitriding and re-oxidation. The model includes the nitriding process under starvation of oxygen and steam and the strongly accelerated process of re-oxidation when oxygen or steam is recovered as observed in several separate effect tests as well as integral experiments. The model distinguishes between two regimes, the breakaway regime at temperatures below 1050 °C and the non-breakaway regime above 1050 °C. In the high temperature regime the acceleration of the oxidation is based on the morphology change due to the nitriding reaction (porous structure of ZrO_2 formed by re-oxidation of ZrN).

Project goals

The presence of nitrogen during the cladding oxidation can lead not only to an acceleration of the cladding degradation by oxygen or steam, but also to enhanced cladding degradation under starvation conditions by the production of ZrN. This will lead to a strong reaction excursion at oxidant recovery because of high reaction rates for zirconium nitride oxidation. Due to the exothermic nature of the ZrN production additional chemical heat is produced and this leads to a temperature increase in the oxygen starved regions. The consumption of the nitrogen also reduces the convectional heat loss by a buoyancy driven air flow in the fuel bundle as observed in the Sandia fuel project [1]. Consequently, adiabatic heat up is a reasonable description of this process.

The *QUENCH-16* experiment [2] showed an unexpectedly high temperature excursion and hydrogen production during the quench phase with water following air ingress with an oxygen starvation phase. The temperature excursion was later explained with the strong re-oxidation reaction of Zr-nitrides produced during the oxygen starvation. The strong effect of nitrogen on the oxidation kinetics of Zircalloy was confirmed in separate effect tests (SETs) especially at *IRSN*, France [3–6] and *KIT*, Germany [7–11]. With an additional experimental program of SETs conducted at *KIT*, with special focus on the discrete stages of pre-oxidation in oxygen, nitriding in nitrogen, and re-oxidation in oxygen, a data base for the development of a nitriding and re-oxidation model was produced. At different temperatures (900 °C, 1000 °C, 1100 °C and 1200 °C) the single stages were investigated with cladding samples of original diameter and material with a length of 10 mm each. Two different thermo-balances were used in more than 70 separate effect tests. The mass gain during the different phases was measured and the samples were also investigated by optical microscopy and with a scanning electron microscope (SEM) after the experiments. All experiments were analysed and the relevant phases for the model development were identified.

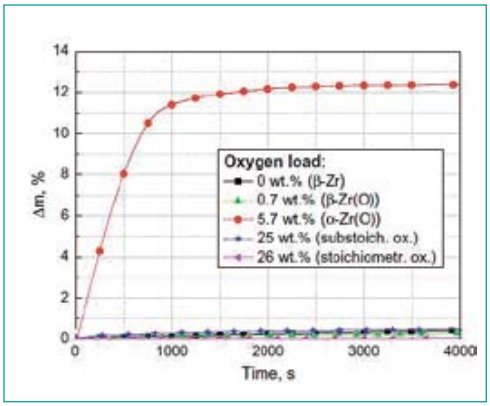

Figure 1: *Nitriding weight gain with different materials taken from [14]*

The goals for this reporting period were:

1) to write a *FORTRAN* subroutine for the calculation of the different processes of nitriding and re-oxidation
2) to develop a standalone computer program with respect to the different gas compositions and changing gas concentrations during uptake and release of oxygen, steam, nitrogen and hydrogen
3) to start the first validation phase with the calculation of SETs and integral experiments
4) to identify areas for further investigation and model improvement

As base of the new nitriding model, the PSI air oxidation model implemented in the *SCDAP/RELAP5* code was used [12]. The new model calculation starts under starvation conditions of oxidants and in the presence of nitrogen. The program logic for the breakaway model is not modified.

Work carried out and results obtained

The new nitriding model describes the different phases of cladding degradation which can occur during a severe accident in a reactor or in a spent fuel pool. Different atmospheric conditions activate different parts of the oxidation and nitriding model. The identification of these phases was important for the understanding of the physical and chemical processes observed during the SETs.

Pre-oxidation

The oxidation of Zircalloy cladding in the pre-oxidation stage is well known based on many investigations in the past [13]. Severe accident codes use different reaction rate functions for different cladding materials and for different gas compositions (air, oxygen, steam). While most of the codes calculate only the production of ZrO_2 the new model also calculates formation of oxygen stabilized alpha zirconium (α-Zr(O)) using the reaction rate function of Leistikow [13]. The reason for the calculation of the production of α-Zr(O) can be seen in Figure 1, which shows the reaction rates of nitrogen with

different materials produced during cladding oxidation. It can be seen that α-Zr(O) is the preferred reaction partner for the nitriding process [14]. Additional to the production of ZrO_2 and α-Zr(O) the temperature dependent breakaway process [12] is calculated to reproduce the higher reaction rates in case of breakaway of the oxide layer. The new nitriding model is activated in the presence of nitrogen and when starvation of the oxidant takes place. Oxidation is calculated if the minimum concentration of the oxidant in the atmosphere exceeds 0.1 %.

Oxygen diffusion

In the absence of steam, oxygen and nitrogen, e. g., in a pure hydrogen atmosphere, the pre-oxidized cladding will undergo a reduction of the Zr-oxide scale due to diffusion of oxygen from the ZrO_2 layer to the zirconium metal. This process is modelled because of the importance of α-Zr(O) for the nitriding reaction. The same production rate function from Leistikow as described above is used for this process and delivers good results for the growing of the α-Zr(O) layer and the coupled decrease of the oxide layer. SETs were carried out at KIT to confirm the oxygen diffusion rate in the absence of oxygen in the carrier gas. In the SETs, the hydrogen atmosphere was replaced by argon to investigate the diffusion rates.

Nitriding

The nitriding process starts when nitrogen is available while steam and oxygen are under starvation conditions or not at all available for the reaction with the cladding material. The temperature dependent reaction rate functions could be deduced from the SETs conducted at *KIT*. The nitriding could be mostly separated into a fast nitriding phase and a slow nitriding phase with a smooth transition in-between. The temperature dependent reaction rates for both reaction mechanisms can be seen in Figure 2 and Figure 3 as Arrhenius plots. In Figure 2 additional reaction rates are included from SETs with α-Zr(O) [14]. In these tests pure α-Zr(O) was used to deduce the (linear) reaction rates in temperature range from 800 °C to 1400 °C. The nitriding rates do not show protective parabolic behavior similar to the pre-oxidation, but linear behavior without changing due to ZrN layer growth. It is assumed, that the structure of the zirconium nitride as well as the formation of non-protective oxide are responsible for a faster gas transport to the reaction front and therefore, the reaction rate

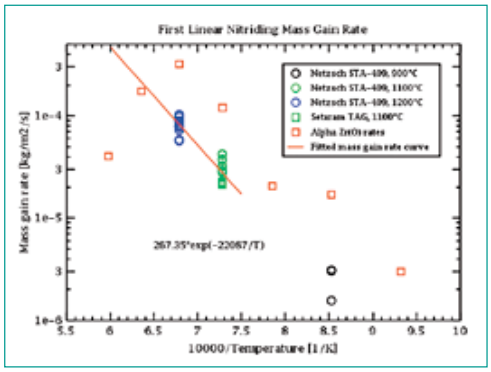

Figure 2:
Fast nitriding rates from SETs at KIT with additional α-Zr(O) rates

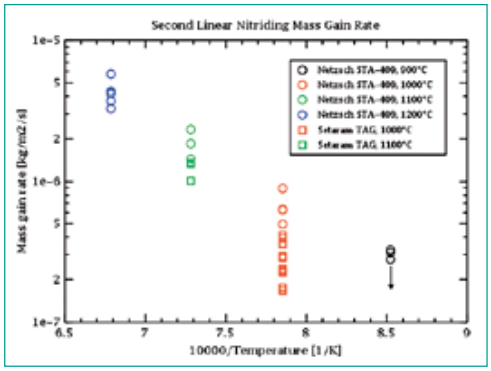

Figure 3:
Slow nitriding rates from SETs at KIT

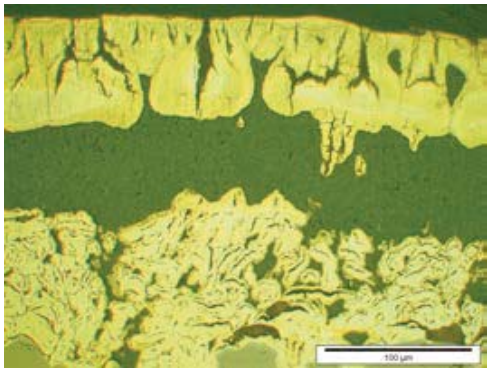

Figure 4:
ZrN layer with ZrO_2 inclusions

stays constant as long as the thickness of the layer is in the order of 1 mm or less. Nitriding is calculated as long as the concentration of nitrogen exceeds 0.1 % in the atmosphere.

The slow nitriding rate is reached after the complete nitriding of the α-Zr(O) layer. The reaction rate then slows down by about a factor of 20. During the consumption of the alpha zirconium layer, it is assumed that the oxygen from the layer is not released from the sample but forms ZrO_2 and new α-Zr(O). The micrographs taken after the nitriding phase showed ZrO_2 inclusions inside the ZrN layer (Figure 4)

Re-oxidation

After the nitriding phase in the SETs, the samples were again oxidized by oxygen. The reaction rates of this oxidation were much higher than those at

the end of the pre-oxidation phase. During the re-oxidation of the ZrN the rates were observed to be about 10 times higher than at the end of the pre-oxidation. For the mass gain, it has to be taken into account that the nitrogen released during the oxidation of ZrN leads to a mass loss of the sample on one side and to a mass gain due to the oxidation on the other side. After oxidation of ZrN has been finished, in a second phase the remaining zirconium metal will be oxidized as well. This second phase is modelled as oxidation after reaching full breakaway conditions as described in [12].

Code validation with SETs

The standalone code is written in a way that temperature, gas composition and gas flow rate are given as input to the oxidation routine and the reaction rates of the different zirconium phases/species are an output of the routine. These data can then be used to calculate the total mass gain which can be compared with the measured data and the results of the micro graphical analysis after the SETs. For comparison with the severe accident code MELCOR a detailed input deck was written to model the Setaram TAG facility which is one of the two facilities used for the SETs. Only the pre-oxidation phase can be compared, because there is no nitriding model available in MELCOR.

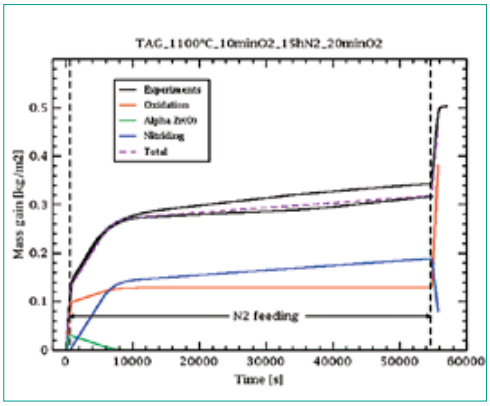

Figure 5: *Mass gain measurement at 1100°C with 10 min O_2, 15 h N_2 and 20 min O_2*

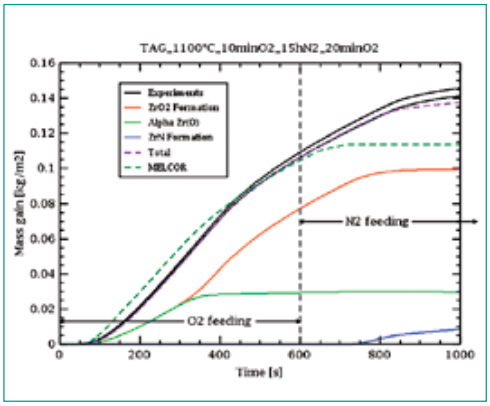

Figure 6: *Mass gain during pre-oxidation of the sample*

The SETs shown below are executed with the Setaram TAG facility with a very leak tight furnace tube and a high accuracy scale at a temperature of 1100 °C. After 10 minutes of pre-oxidation, a nitriding phase of 15 hours was carried out followed by a re-oxidation phase of another 20 minutes. As can be seen, the mass gain calculated for the experiments with the standalone code is in good agreement with the experimental data (Figure 5) in all phases of the SETs.

Figure 6 shows the calculated mass gain curves from MELCOR and the standalone code for the phase of the pre-oxidation. In these tests the pre-oxidation time was 600 seconds. After switching on the gas flow it needed about 40 seconds for the reacting gas to reach the position of the sample due to the slow mass flow and the facility geometry. Another 250 seconds passed until the steady state concentration of the oxygen was reached at the sample position (Figure 7). These concentrations are deduced from experimental measurements. After 600 seconds of pre-oxidation the reacting gas was changed from oxygen to nitrogen to start the nitriding process. The concentration of the reacting gases before and after the sample position in the experimental facility (Figure 7) shows the consumption of almost all the oxygen (starvation) at the beginning of the experiment until about 350 seconds. From this time until about 750 seconds the oxidation is running under non-starved conditions, even after switching of the gas source from oxygen to nitrogen. After reaching starvation conditions under presence of nitrogen the nitriding reaction is starting.

The mass gain rate calculated by the standalone code for the two experiments, one with pre-oxidation and nitriding and the other additionally with re-oxidation, is in very good agreement with the experimental values for all phases of the SETs (Figures 8, 9 and 10). The MELCOR calculation did not cover the beginning of the test because of the modelling of the facility with a small number of volumes (there is only one gas concentration set for every volume). The MELCOR calculation also consumes only up to 90 % of the available oxygen, while the standalone program is consuming all the available oxygen as long as the oxygen flow rate remains smaller than the oxygen consumption rate defined by the reaction rate. The mass gain during the nitriding phase (Figure 9) could also be calculated in very good agreement with the experimental data. The fast nitriding reaction with the consumption of the α-Zr(O) as well as the transition

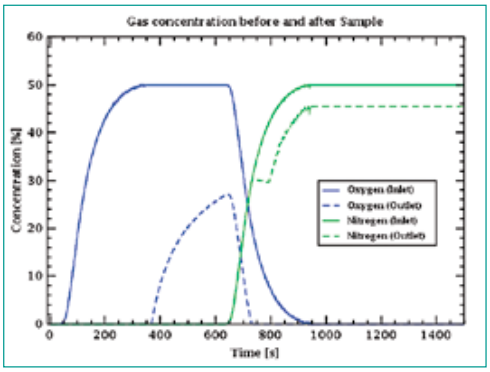

Figure 7: *Concentration of the reacting gases before and after the sample position*

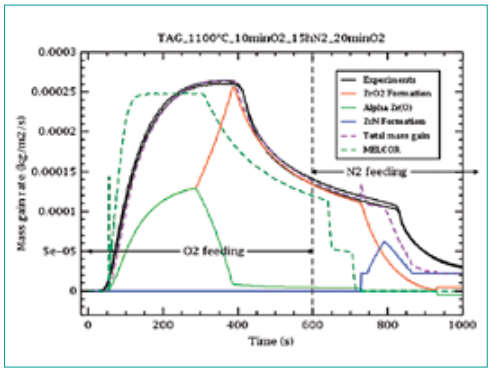

Figure 8: *Mass gain rate during pre-oxidation of the sample*

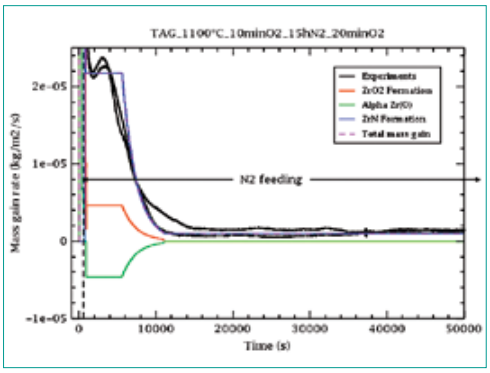

Figure 9: *Mass gain rates during nitriding phase*

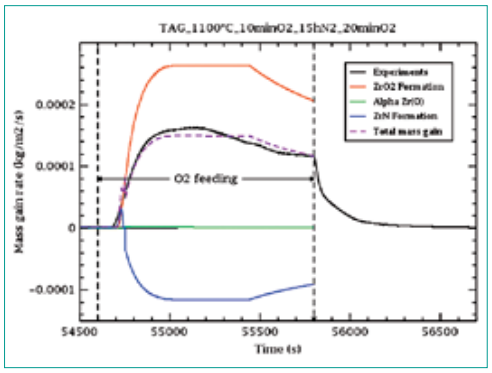

Figure 10: *Mass gain rate during re-oxidation phase*

to the slow nitriding reaction are fitting the data. During the re oxidation (Figure 10), the consumption of ZrN and the production of ZrO_2 with the resulting total mass gain rate are shown to agree with the experimental data.

Sandia fuel project: Phase II

In an earlier ENSI research project [15] the OECD SFP experiment phase II [1] was investigated. As a result of the investigation the open question of the influence of nitriding reactions on the experiment progression was identified. With the standalone program described above, oxidation and nitriding reactions during the cladding degradation were calculated using the temperature and mass flow data calculated with MELCOR. The model of the 1 × 4 fuel assembly experiment (1 heated assembly in the centre and 4 cold fuel assemblies around) was represented by a seven ring model horizontally and with 12 vertical nodes along the active length of the fuel assemblies (FAs). The FAs were standard 17 × 17 rods PWR fuel assemblies with original materials except for the fuel which was simulated by MgO pellets with electrical heating. The cooling of the FAs was performed through buoyancy driven air flow to simulate a spent fuel pool after loss of coolant. After heat up due to the electrical heating of the centred FA the cladding ignited at about 1200 K in the vertical node 10 in the centre of the heated FA. Then the zirconium fire propagated first downward and after complete oxidation of the cladding in the lowermost nodes it propagated upwards again until all the cladding was oxidized. During the downward propagation of the zirconium fire all thermo couples (TCs) failed after passing of the fire front. Also, the gas flow measurement device at the inlet of the bundle was destroyed by molten aluminium from the neutron absorbers (borated aluminium plates). Only the off-gas measurement was functioning until the end of the experiment. Figure 11 shows the temperature of two nodes below the ignition point calculated by MELCOR. The calculation is in good agreement with the experimental data until failure of TCs at ignition of the cladding at the TC position. After the zirconium fire passed the nodes the temperature decreased in the calculation because of oxygen starvation and therefore missing chemical energy. The increase of the chemical energy due to the nitriding reaction under partial or full oxygen starvation conditions is shown in Figure 12. This indicates that the calculated temperatures after the first

maximum are too low because of the missing nitriding energy. The «nuclear power» shown in figure 12 represents the electric heating power in this node until failure of the heating device shortly after ignition of the zirconium fire.

The off-gas data (Figure 13) indicate that the consumption of nitrogen in the oxygen starved region of the FAs led to a counter current gas flow from above. Each vertical line in Figure 13 represents ten hours in the experiment. It can be seen that after ignition at about 6 hours, the oxygen flowrate dropped to zero and at about ten hours it suddenly «recovered». This oxygen «recovery» can be explained by the consumption of nitrogen between 10 and 15 hours which led to an almost stagnant gas flow in the FA (Figure 14) if the nitriding model is used. This almost stagnant gas flow from below allows a counter current gas flow from above carrying oxygen to the bundle enabling the measurement of oxygen in the «off-gas».

When the zirconium fire reaches the lowermost nodes at about 15 hours the counter current gas flow was stopped (Figure 13) and the oxidation front started to move upwards to oxidize the produced ZrN and remaining metal. This leads to the release of nitrogen and a thereby increased gas flow of nitrogen at the outlet (Figures 13 and 14). The nitrogen consumption calculated by the standalone program between 30 hours and 50 hours (Figure 14) is because of the too low temperatures after the ignition in the upper region calculated by the MELCOR code (Figure 11) without including the nitriding process. After failure of the TCs and the inlet gas flow device the comparison of the calculation with the experiment can only be done in a qualitative way. The mass balance from the released nitrogen due to the off-gas analysis in the late phase indicated the nitriding of a large amount of the non-oxidized metal left during zirconium fire downward propagation.

The strong influence of the nitriding reaction on the thickness of the remaining metal layer is shown in Figure 15 and Figure 16. Without considering the nitriding reaction the metallic cladding survives the zirconium fire during the downward propagation as calculated by MELCOR (Figure 15) until 60 hours for node 6 and 70 hours for node 8 when the fire propagates upwards again and oxidises the remaining metal.

The standalone code has no material property package and no heat radiation and conduction models and therefore the enhanced temperatures due to the nitriding reactions and the reduced convectional heat loss cannot be calculated. The temperature drop (Figure 11) after ignition calculated by MELCOR lead to a reduced nitriding reaction of the cladding in node 8, about half a meter below the first ignition point (Figure 16). At about 25 hours MELCOR calculates increasing temperatures due to the oxidation front coming closer to node 8 during the upward propagation of the zirconium fire. With these increasing temperatures the standalone code now calculates increasing nitriding rates and a complete nitriding of the cladding at about 33 hours. Shortly after 50 hours the oxidation front reaches node 8 and then oxidises the ZrN until 58 hours. The process of the nitriding in this node would have happened earlier if the temperature calculation would have taken the nitriding energy into account. The higher temperatures in node 6 (Figure 11) lead to a complete consumption

Figure 11: *Temperatures of two nodes below ignition point*

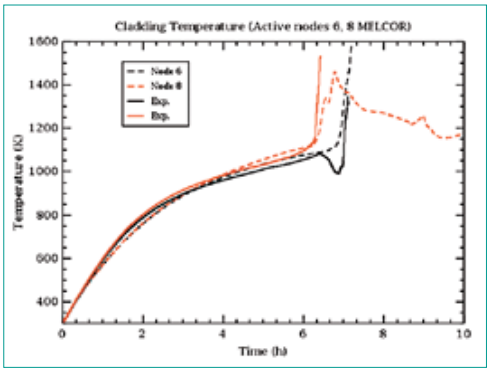

Figure 12: *Chemical power produced in active node 6*

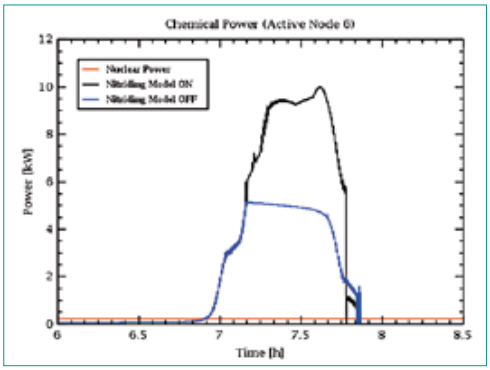

Figure 13: *Off-gas measurement of SFP phase II experiment [1]*

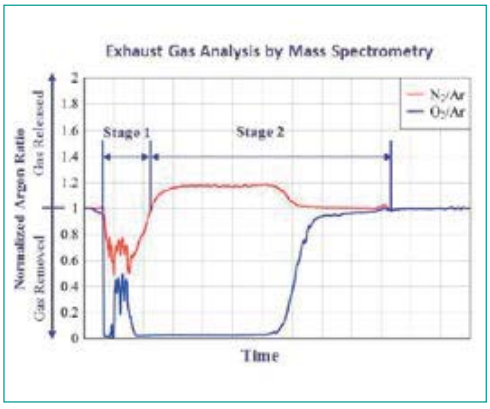

of the zirconium metal at 8 hours due to the additional nitriding instead of almost 60 hours as in the MELCOR calculation without nitriding.

National Cooperation

At the national level the results will be implemented into projects with both ENSI and swissnuclear for application to safety analyses of the Swiss nuclear power plants. The national partners are regularly informed about the results of the project.

International Cooperation

In close collaboration with KIT in Germany, additional data sets from earlier experiments (SETs and QUENCH experiments) were used for the further validation of the nitriding model. For the implementation of the nitriding model into severe accident codes, contacts have been made with the SCDAPSim code developers (ISS) as well as with Sandia National Laboratories (MELCOR) and the US NRC. Results of the project are presented in different meetings with the partners.

Assessment 2018 and Perspectives for 2019

In 2018, a standalone computer code was written for the developing and the testing of the new cladding degradation subroutine. The model developed during the year 2018 was implemented into the existing air oxidation and breakaway code [12] and tested successfully with separate-effect tests and the Sandia fuel project phase II. Areas for further validation were identified especially in the low temperature range below 1300 K because of the breakaway effect and in the temperature range above 1600 K because of the reduction of the reaction rate between α-Zr(O) and nitrogen [14].
Additional data sets from experiments (SETs and QUENCH experiments) conducted at KIT in Germany will be used to update the nitriding model for calculations in the extended temperature region below 1300 K and above 1600 K. Validation calculations will be prepared for other large scale experiments and the code will be prepared and described for the implementation into severe accident codes like MELCOR and SCDAPSim.

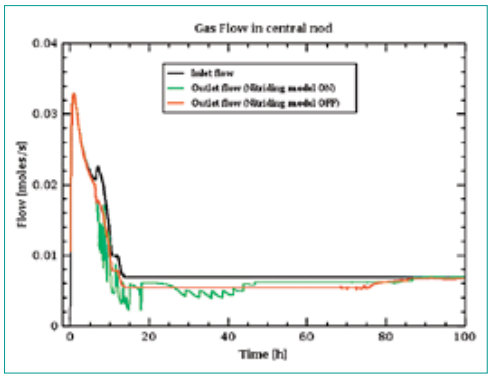

Figure 14:
Gas flow calculation at the outlet of the inner ring

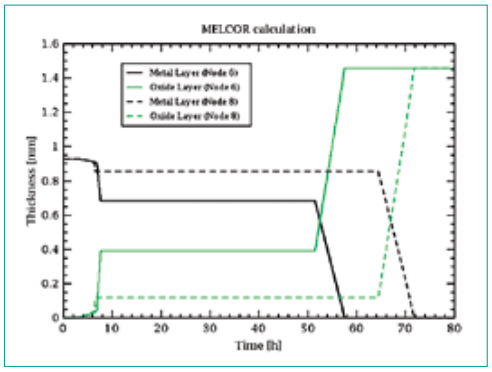

Figure 15:
Thickness of material layers calculated by MELCOR

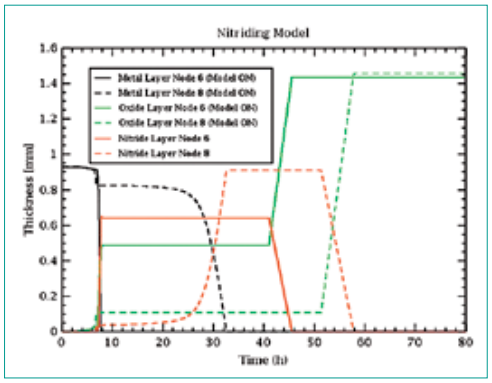

Figure 16:
Thickness of material layers calculated by standalone code

Publications

- *B. Jäckel, T. Lind, L. Fernandez-Moguel, M. Steinbrück, S. Park,* Development of a computer code model for nitriding and re-oxidation of cladding materials under severe accident conditions. 27th NENE Conference, Portorož, Slovenia, September 10–13, 2018.
- *B. Jäckel, L. Fernandez-Moguel, T. Lind, S. Park, M. Steinbrück,* PSI-KIT nitriding model with validation calculations. 24th QUENCH workshop, Karlsruhe, Germany, November 13–15, 2018.

References

[1] *S. G. Durbin et al*, Spent Fuel Pool Project Phase II, NUREG/CR-7216, US-NRC, 2016.

[2] *J. Stuckert, M. Steinbrück,* Experimental results of the QUENCH-16 bundle test on air ingress, Progress in Nuclear Energy 71, 134–141, 2014.

[3] *M. Lasserre, V. Peres, M. Pijolat, O. Coindreau, C. Duriez, J.-P. Mardon,* Modelling of Zircaloy-4 accelerated degradation kinetics in nitrogen-oxygen mixtures at 850 °C, Journal of Nuclear Materials 462, 221–229, 2015.

[4] *M. Lasserre, V. Peres, M. Pijolat, O. Coindreau, C. Duriez, J.-P. Mardon,* Qualitative analysis of zircaloy-4 cladding air degradation in O2-N2 mixtures at high temperatures, Materials and Corrosion 65, 250–259, 2014.

[5] *C. Duriez, D. Drouan, G. Pouzadoux,* Reaction in air and in nitrogen of pre-oxidised Zircaloy-4 and M5™ claddings, Journal of Nuclear Materials 441, 84–95, 2013.

[6] *C. Duriez, M. Steinbrück, D. Ohai, T. Meleg, J. Birchley, T. Haste,* Separate-effect tests on zirconium cladding degradation in air ingress situations, Nuclear Engineering and Design 239, 244–235, 2009.

[7] *M. Steinbrück, F. O. da Silva, M. Grosse,* Oxidation of Zircaloy-4 in steam-nitrogen mixtures at 600–1200 °C, Journal of Nuclear Materials 490, 226–23, 2017.

[8] *M. Steinbrück, S. Schaffer,* High-Temperature Oxidation of Zircaloy-4 in Oxygen-Nitrogen Mixtures, Oxidation of Metals 85, 245–262, 2016.

[9] *M. Steinbrück, M. Grosse,* Deviations from parabolic kinetics during oxidation of zirconium alloys, ASTM Special Technical Publication STP 1543, 979–1001, 2015.

[10] *M. Steinbrück, M. Böttcher,* Air oxidation of Zircaloy-4, M5® and ZIRLO™ cladding alloys at high temperatures, Journal of Nuclear Materials 414, 276–285, 2011.

[11] *M. Steinbrück,* Prototypical experiments relating to air oxidation of Zircaloy-4 at high temperatures, Journal of Nuclear Materials 392, 531–544, 2009.

[12] *J. C. Birchley, L. Fernandez-Moguel,* Simulation of air oxidation during a reactor accident sequence: Part 1 – Phenomenology and model development, Annals of Nuclear Energy 40, 163–170, 2012.

[13] *G. Schanz, B. Adroguer, A. Volchek,* Advanced treatment of zircaloy cladding high-temperature oxidation in severe accident code calculations Part I. Experimental database and basic modelling, Nuclear Engineering and Design 232, 75–84, 2004.

[14] *M. Steinbrück,* High-temperature reaction of oxygen-stabilized a-Zr(O) with nitrogen, Journal of Nuclear Materials 447, 46–55, 2014.

[15] *J. C. Birchley, L. Fernandez-Moguel, A. Rydl, B. Jäckel,* Code Assessment Program for MELCOR 1.8.6, ENSI Erfahrungs- und Forschungsbericht, 225–232, 2012.